

The sinus of Valsalva relieves abnormal stress on aortic valve leaflets by facilitating smooth closure

Susumu Katayama, BE, Nobuyuki Umetani, BE, Seiryō Sugiura, MD, PhD, and Toshiaki Hisada, PhD

Objective: Recently, various modifications have been made to aortic root replacement procedures to include the pseudosinus in the synthetic graft, but its effect on valve function still remains to be elucidated. The purpose of this study was to compare the flow dynamics and its influence on the stress/strain in the valve leaflet in two types of aortic root, either with or without the pseudosinus, with a simulation model.

Methods: The proximal portions of the ascending aorta and aortic valves were modeled with blood flowing inside. Blood flow and the motion of aortic valve leaflets were studied while applying a physiologic pressure waveform using fluid–structure interaction finite element analysis. Waveforms were varied to simulate the change in cardiac contractility.

Results: In the aorta without the sinus, the time during which the valve was open was longer and the rapid valve closing velocity was faster under all conditions studied. In the pseudosinus model, we could clearly observe vortex formation from the early phase of ejection, which seemed to facilitate the gradual but smooth closure of the valve. Valve leaflets without the sinus were subject to greater stress and underwent bending deformation in the longitudinal direction.

Conclusions: Sinuses of Valsalva facilitate the smooth closure of the aortic valve, thereby avoiding the building up of abnormal stress in the leaflet. Such an effect may assure the durability of valve leaflets in aortic grafts with a pseudosinus.



Video clip is available online.



Supplemental material is available online.

Sinuses of Valsalva, with their characteristic morphologic features, have attracted the interest of researchers, and earlier modeling studies have suggested that the sinuses function not only to prevent the contact of valve leaflet with the aortic wall, but also to facilitate valve closure by the formation of vortices inside them.^{1,2} The emergence of valve-sparing aortic root replacement procedures for the treatment of patients with aortic root disease has provided us with the unique opportunity to test such hypotheses. Leyh and colleagues³ compared patients who had undergone tube replacement of the aortic root (reimplantation [David I] procedure) and

those who had undergone separate replacement of the sinuses of Valsalva (remodeling [Yacoub] procedure) to find that the near-normal opening and closing characteristics of valves were achieved by the preservation of the shape and independent mobility of the sinuses. On the other hand, de Oliveira and associates,⁴ based on a decade of following up surgically treated patients, reported a reduced risk of postoperative aortic insufficiency in patients with reimplantation. They concluded that the implantation procedure secures the entire aortic valve inside the Dacron graft to prevent dilatation of the aortic root and concomitant regurgitation. However, they also recognized the elimination of sinuses as a shortcoming of their technique, and they, as well as other surgeons, have modified their reimplantation techniques to create graft pseudosinuses.⁵⁻⁷

Although it is generally assumed that smooth opening and closing relieved the abnormal stress and strain on leaflets, neither clinical observations^{3,8-10} nor experimental studies using a mock circulation^{11,12} could provide us with detailed information on the stress and/or strain distribution in the leaflet to clarify this assumption. An alternative approach to overcome such technical difficulty and obtain stress and strain distribution is a simulation study using finite element analysis. Grande-Allen and associates¹³ created finite element models of the aortic root and valve with a cylindrical graft, a tailored graft sutured just above the valve, and a pseudosinus graft, to find that the cylindrical graft created the greatest stress. Beck, Thubrikar, and Robicsek¹⁴ also compared the finite element models of the tubular aortic root and the root with sinuses under pressure to find that a stress concentration along the leaflet attachment develops only in

From the Department of Human and Engineered Environmental Studies, Graduate School of Frontier Sciences, The University of Tokyo, Kashiwa-shi, Chiba, Japan. This study was supported by Core Research for Evolutional Science and Technology (CREST) program by Japan Science and Technology Agency (JST). Received for publication Feb 25, 2008; revisions received April 22, 2008; accepted for publication May 19, 2008.

Address for reprints: Seiryō Sugiura, MD, PhD, Department of Human and Engineered Environmental Studies, Graduate School of Frontier Sciences, The University of Tokyo, 5-1-5 Kashiwa-no-ha, Kashiwa-shi, Chiba, Japan (E-mail: Sugiura@k.u-tokyo.ac.jp).

J Thorac Cardiovasc Surg 2008;136:1528-35
0022-5223/\$34.00

Copyright © 2008 by The American Association for Thoracic Surgery
doi:10.1016/j.jtcvs.2008.05.054

Abbreviations and Acronyms

ALE	= arbitrary Lagrangian–Eulerian
C	= cylindrical graft
DOF	= degree of freedom
P	= pseudosinus graft
P90	= peak pressure of 90%
P100	= control peak pressure
P110	= peak pressure of 110%
RVCV	= rapid valve closing velocity
SCD	= slow closing distance

the tubular root. Although these studies gave strong support to surgeons' beliefs, the simulation was done only by applying pressure to the model, thus totally ignoring the influence of the blood flow, which most of the surgeons and researchers are interested in. The capabilities of the fluid–structure interaction finite element method for the analysis of the aortic valve were first shown by Nicosia and colleagues¹⁵ using a commercial software package; subsequently, de Hart and coworkers¹⁶ analyzed the normal aortic root using the fictitious domain method. However, owing to the numerical instability of the method, an unphysiologically low Reynolds number flow was introduced.

We¹⁷ have developed a numerical approach for fluid–structure interaction analysis based on the arbitrary Lagrangian–Eulerian (ALE) finite element method and applied it to the multiphysics simulation of the heart.^{18–21} In this study, we applied this method to the analysis of the dynamics of aortic valve opening and closure in two different models of the aortic root, with or without the sinuses of Valsalva. It will be clearly shown that the sinuses, by promoting vortex formation, facilitate the smooth closure of the aortic valve and circumvent the development of abnormal stress in the leaflets.

METHOD

Modeling the Aortic Root

We created the shapes of cylindrical graft and pseudosinus graft with the dimensions shown in Figure 1, A. Then, we modeled the blood domain by tetrahedral finite elements with four velocity nodes and four pressure nodes, resulting in the total numbers of elements and the degree of freedom (DOF) of 4408 (24990 DOF) for the cylindrical model and 52620 (30658 DOF) for the pseudosinus model. For the valve leaflets, we adopted discrete Kirchhoff triangular shell elements with anisotropic material property originating from the fiber orientation^{15,22} (Figure 1, B). Furthermore, the edge of each leaflet was made thicker according to the literature.²³ For the material properties of the valve, see Table E1.

The Heart and the Systemic Circulation as Boundary Conditions

To the distal end of the models, we connected the 3-element Windkessel model of systemic circulation. Pumping function of the heart was simulated by applying the physiologic pressure wave (minimum 75 mm Hg, maximum 120 mm Hg). To simulate cases in which contractility of the heart is

either depressed (heart failure) or augmented, we varied the peak pressure to 90% (P90) or 110% (P110) of the control (P100) condition while keeping the pressure time products constant (Figure 1, C). This was intended because we usually observed a slowed time course of contraction when the contractility was depressed.

Computation

We used a strongly coupled fluid–structure interaction finite element analysis program, which we have developed¹⁷ and applied to various problems such as pulsation of the heart.^{18–21} In this program, the Navier–Stokes equation is described in ALE coordinates, which artificially deform and move according to the instantaneous deformation of the fluid–structure interface. Furthermore, the fluid meshes and structure meshes are generated to coincide with each other on the interface at the beginning of the analysis. Therefore, the geometric compatibility and balance of traction forces are automatically satisfied by merging both meshes on the interface. The disadvantage of the method is the distortion of ALE meshes. Because the fluid–structure interface moves largely in the case of a heart valve problem, excessive ALE mesh distortion occurs, resulting in the degradation of element performance. To avoid such a problem, we applied an automatic mesh reconnecting algorithm, which our group has developed. All of the program codes were written in the laboratory.

RESULTS

The flow dynamics and the motion of the valves in cylindrical and pseudosinus grafts can be seen in the online supplementary [Movies E1 and E2](#). In the pseudosinus graft, we can clearly observe the formation of vortices of counter-clockwise rotation in the sinuses, which seems to facilitate the closure by pushing the leaflets. In the cylindrical graft, the edges of the leaflets make contact with the wall when they are fully open and the closure seemed to be retarded. Peak velocity values were 0.95 m/s (P90), 1.04 m/s (P100), and 1.16 m/s (P110) and the corresponding Reynolds numbers were 2995, 3278, and 3657, respectively.

Motion of the Leaflets

To quantify the motion of the leaflets and compare the simulation results with clinical observations, we traced the edge of the leaflet and plotted the distance from the axis of the aorta as a function of time, as we do in M-mode echocardiography (Figure 2, A), and calculated the slow closing distance (SCD = $[D1 - D2]/D1$) and closing time (Figure 2, B). SCD values were greater for pseudosinus models (P) than for cylindrical models (C) under all of the conditions studied, but the difference was pronounced in response to low ejecting pressure (P vs C [%]: 8.9 vs, 5.1 [P110], 7.7 vs 4.6 [P100], and 6.3 vs 0.6 [P90]) (Figure 3, A). On the contrary, although the differences were small, closing time tended to be longer with the cylindrical model (P vs C [s]: 0.22 vs 0.24 [P110], 0.24 vs 0.25 [P100], and 0.26 vs 0.28 [P90]) (Figure 3, B). We also calculated the rapid valve closing velocity (RVCV) as the ratio between D2 and rapid closing time (RCT in Figure 2, B). RVCV was also faster for cylindrical models (P vs C [cm/s]: 50.6 vs 52.1 [P110], 49.8 vs 58.5 [P100], and 30.8 vs 42.7 [P90]) (Figure 3, C). These results can be taken to indicate that, in the presence

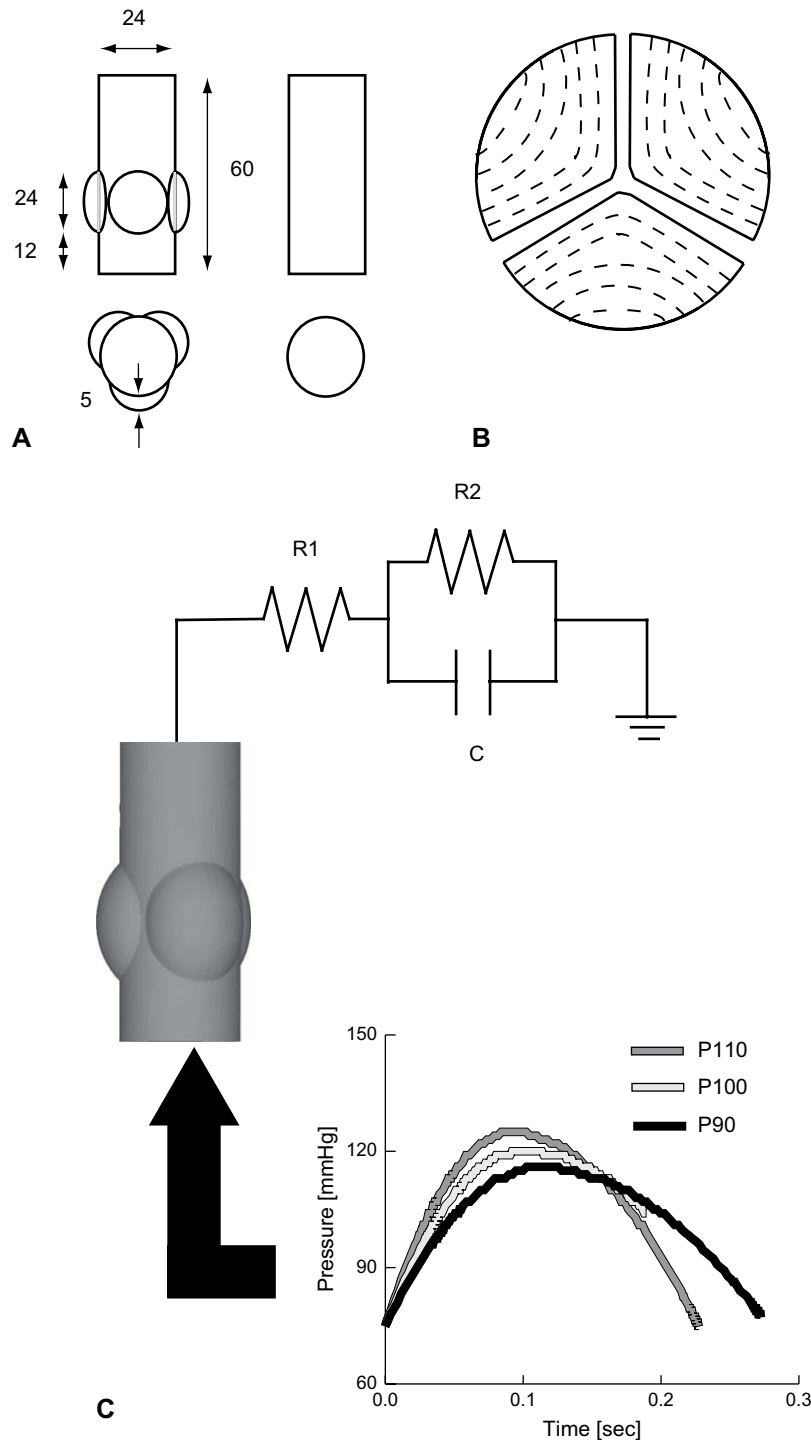


FIGURE 1. Configurations of the model. A, Cylindrical (*left*) and pseudosinus (*right*) aortic roots with details of their dimensions. B, Valvular leaflet and fiber orientation (*right*). C, Simulated aortic pressure was applied to the proximal end of the model aortic root. To the distal end, a 3-element Windkessel model was connected. *R1*, Characteristic impedance ($100 \text{ dynes} \cdot \text{s} \cdot \text{cm}^{-5}$); *R2*, peripheral resistance ($1600 \text{ dynes} \cdot \text{s} \cdot \text{cm}^{-5}$); *C*, capacitance ($2.1 \times 10^{-3} \text{ L/mm Hg}$).

of pseudosinuses, the valvular leaflets initiate their motion from the earlier phase of ejection and gradually return to their closing positions. On the other hand, with the cylindrical model, valves are wide open until the late phase

of ejection, during which the flow direction is reversed to increase the regurgitant fraction (P vs C [%]: 0.7 vs 4.4 [P110], 1.6 vs 4.2 [P100], and 0.4 vs 5.4 [P90]) (Figure 3, D).

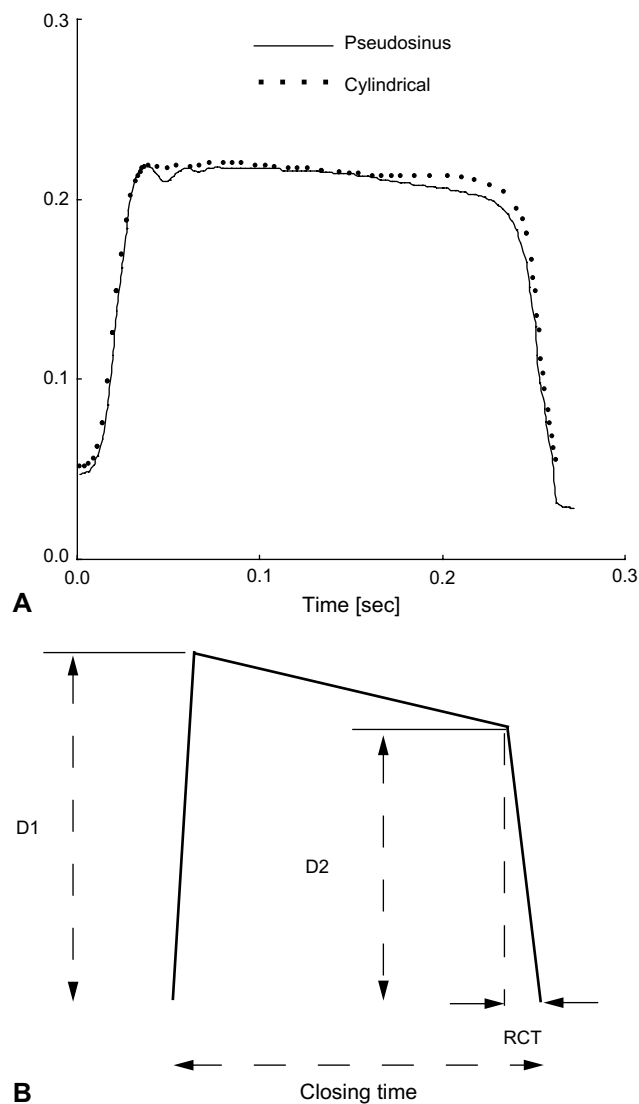


FIGURE 2. Motion of the leaflet. A, The distance from the axis of the aorta is shown as a function of time. *Solid line*, Pseudosinus model; *dotted line*, cylindrical model. B, Schematic diagram showing the indices characterizing the motion of leaflet. *D1*, Maximum distance; *D2*, distance immediately before the rapid closing. *RCT*, Rapid closing time.

Strains and Stresses in the Leaflets

We also compared the strains and stresses in the leaflets between the two models. Taking into consideration the anisotropic material property reflecting the fiber orientation and the complex deformation each leaflet undergoes during the ejection, we calculated the peak stretch (membrane), bending, and total strains (ϵ) parallel ($||$) and perpendicular (\perp) to the fiber orientation. As shown in Figure 4, A, the leaflets in the cylindrical model experience greater peak strains, especially in the direction perpendicular to the fiber orientation (C vs P: 0.022 vs 0.012 [membrane $\epsilon_{||}$], 0.042 vs 0.024 [membrane ϵ_{\perp}], 0.069 vs 0.069 [bending $\epsilon_{||}$], 0.087 vs 0.064 [bending ϵ_{\perp}], 0.065 vs 0.060 [total $\epsilon_{||}$], 0.089 vs 0.068 [total-

ϵ_{\perp}]). Interestingly, the bending strains in the fiber direction did not differ appreciably between the two models. Comparison of peak stress (σ) values followed similar pattern to the strain values (C vs P [kPa]: 15.9 vs 8.6 [membrane $\sigma_{||}$], 9.8 vs 5.6 [membrane σ_{\perp}], 48.0 vs 48.1 [bending $\sigma_{||}$], 20.3 vs 14.8 [bending σ_{\perp}], 45.3 vs 41.8 [total $\sigma_{||}$], 20.8 vs 15.7 [total σ_{\perp}]) (Figure 4, B).

DISCUSSION

In this study, we applied the fluid–structure interaction finite element method to analyze the flow dynamics in the aortic root and the motion of the aortic valve. Comparison of two models with or without the sinuses of Valsalva clearly demonstrated their functional role in achieving the smooth closure of the valves. These results also have relevance to aortic root surgery, modifications to the procedures for which have been proposed to improve the prognoses of patients.

Simulations of Aortic Root

Compared with studies using mock circulation,^{1,11,12} simulation studies using the finite element method have advantages in that (1) the shape and the material properties of the model and experimental conditions can be altered and controlled over a wide range, (2) detailed data on the distribution of flow velocity and pressure are available, and (3) stress/strain distribution in the aortic wall and/or valvular leaflet can be calculated. In particular, stress data are important but hard to obtain in clinical settings.

However, so far, we can find only a few simulation studies in which fluid–structure interactions were analyzed, probably owing to the computational difficulties.^{15,16,24} Among these studies, Nicosia and colleagues¹⁵ constructed an anatomically accurate 3-dimensional finite element model in which both the aortic root and valves were represented by Hughes–Liu shell elements. They analyzed the blood flow and the motion of the valve leaflet during ejection by using LS-Dyna—an explicit finite element commercial code. Their pioneering work showed the potential capabilities of the fluid–structure finite element analysis for heart valve problems. However, some unphysiologic conditions, such as the 98.5% reduction in the bending stiffness of the valve leaflets, were introduced to reproduce their pliability, which in turn enforced the scaling down of the magnitude of the peak diastolic pressure to avoid valve element distortion. After Nicosia and colleagues,¹⁵ de Hart and associates,¹⁶ using the fictitious-domain method, successfully showed that vortex formation in the sinuses of Valsalva is essential for the smooth operation of the aortic valve. In contrast to the present study, however, their computation was carried out with an unphysiologically low Reynolds number (~ 900) owing to the numerical instabilities inherent in the algorithm.

Furthermore, a comparison of two clinically relevant models, namely, cylindrical and pseudosinus, based on fluid–structure interaction analysis, has been made for the

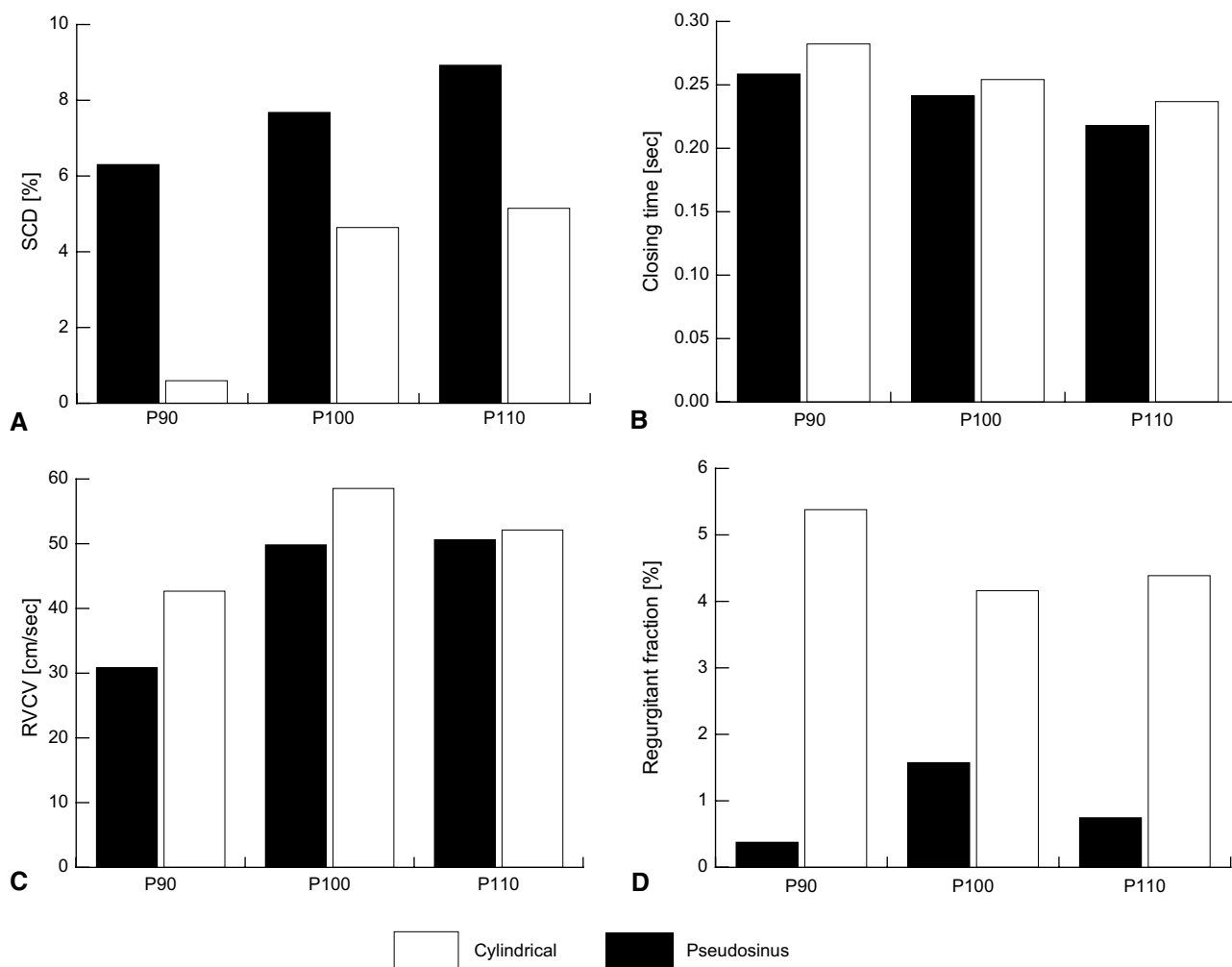


FIGURE 3. Comparison of valve functions. A, Slow closing distance (*SCD*). B, Closing time. C, Rapid valve closing velocity (*RVCV*). D, Regurgitant fraction. *White bar*, Cylindrical model; *black bar*, pseudosinus model.

first time. Although we can find the finite element analysis studies comparing the principal tensile stress of leaflets between the cylindrical graft and pseudosinus graft,^{13,14} in those study, the calculation was carried out for only the diastolic period by applying the pressure, thus completely ignoring the influence of blood flow.

Comparison With Experimental and Clinical Studies

Using the time-resolved 3-dimensional magnetic resonance velocity mapping, Markl and associates¹⁰ compared vortex formation among patients who had undergone cylindrical graft (David I procedure) and those who had undergone neosinus graft (David V and David V-S_{mod} [Stanford modification]), with normal volunteers as controls. Even though vorticity was increased in patients who underwent the David V procedure, because the difference did not reach statistical significance, they concluded that, although vortex formation was enhanced by the David V procedure, normal vorticity was preserved even without the sinus creation in

the graft. Direct comparison with the current simulation results is difficult, because in this study a rigid tube with perfect cylindrical form was used, but a small degree of vortex formation was also identified in our simulation (*Movie E2*).

In a study comparing the motion of the leaflets between the patients who had undergone tube graft and those who had undergone remodeling (Yacoub) procedure, Leyh and coworkers³ reported that, in patients who had undergone remodeling, *SCD* was greater but closing time was shorter, consistent with the present results. A similar tendency was reported for the comparison between patients with a tube graft and those with a newly developed graft with a pseudosinus.⁸ However, the *RVCV* differed between the two studies. Leyh and coworkers³ found that the *RVCV* was slower for tube grafts, but De Paulis and associates⁸ reported results to the contrary.

In vitro studies may help to resolve this discrepancy. Fries and coworkers¹¹ placed a porcine aortic root operated on with either the David (cylinder) or Yacoub (remodeling) procedure

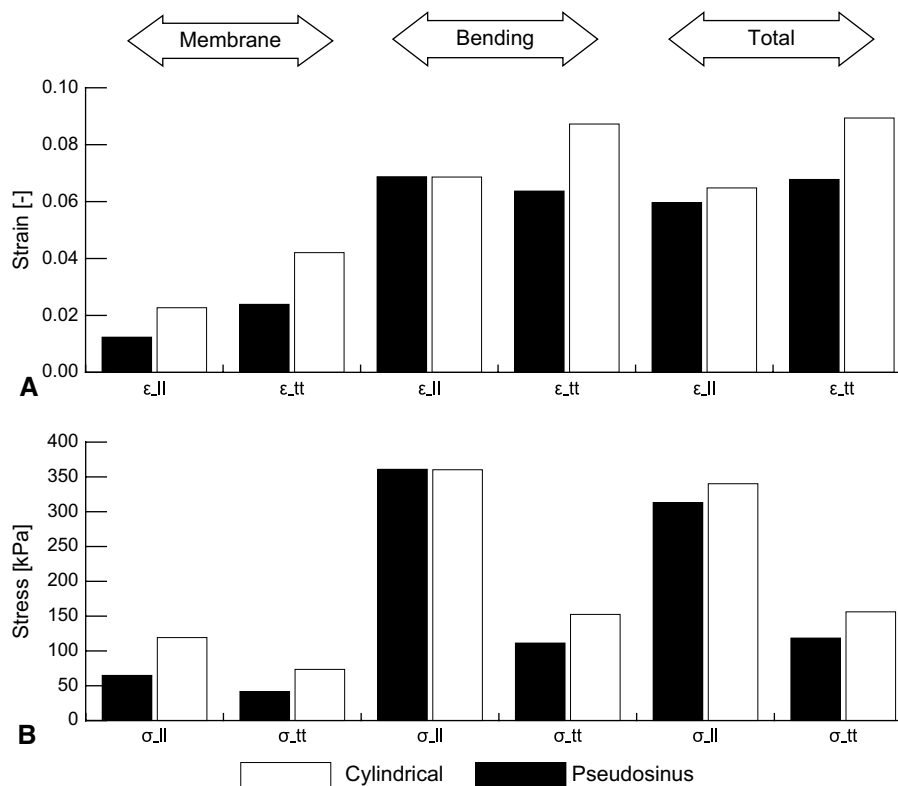


FIGURE 4. Strain and stress in the leaflet. A, Strain (ϵ). B, Stress (σ). Values for membrane (tensile), bending, and total are shown in parallel (||) and perpendicular (tt) to the fiber direction. *White bar*, Cylindrical model; *black bar*, pseudosinus model.

in a mock circulation and recorded the motion of the valve. The difference in SCD was similar to the clinical observation mentioned above, as well as the present results, but they found that the differences in RVCV were dependent on cardiac output and that the RVCV was greater for the David procedure only at low cardiac output, similar to the present result (Figure 3, C). These contradictory results may have arisen because the patients in the study by Leyh and colleagues³ had relatively high cardiac function (ejection fraction > 60%) compared with patients in other studies (about 50%).

As we mentioned earlier, the stresses and/or strains in the leaflet during ejection are hard to measure, but there has been a study in which strains were compared among the various surgical procedures.¹² From the images of porcine aortic roots operated on differently and placed in the mock circulation, the authors of this study calculated the cusp-bending deformation index in mid-systole as the fold depth normalized to the size of the leaflet. Although the index of strain used in this study was just an estimate, their results demonstrated a greater strain associated with the reimplantation procedure (tube graft), compatible with our simulation result.

Implications

Although the creation of sinuses in remodeling procedures introduces the smooth closure of the aortic valve,³

a long-term follow-up study demonstrated a better prognosis for patients undergoing the reimplantation (David I) procedure in terms of freedom from aortic regurgitation,⁴ mainly because of the more reliable annular stabilization with this technique. However, the importance of the sinuses of Val-salva is widely recognized by cardiac surgeons, and various modifications to the reimplantation procedure have been proposed to achieve both annular stability and the creation of sinuses.^{6-8,25,26} Although these techniques are expected to enhance the long-term durability of the leaflet, greater knowledge of the functional anatomy of the aortic root is required to achieve optimal results.²⁷ The current simulation would serve as a useful tool for designing tailor-made aortic grafts and, in fact, has provided us with new insight into the mechanics of the aortic valve leaflet during ejection.

Shown in Figure 5, A, are the stress distributions in the leaflets during the late phase of ejection for pseudosinus (*upper panel*) and cylindrical (*lower panel*) grafts (Movie E3). It can clearly be seen that the leaflet in the cylindrical graft is bent in its middle portion by being pushed by the retrograde flow from both sides (Movie E4). On the other hand, the leaflet in the pseudosinus graft has already returned halfway to the closed position, as evidenced by the large SCD, and accommodates the retrograde flow only on one side to avoid the abnormal bending stresses perpendicular to the fiber

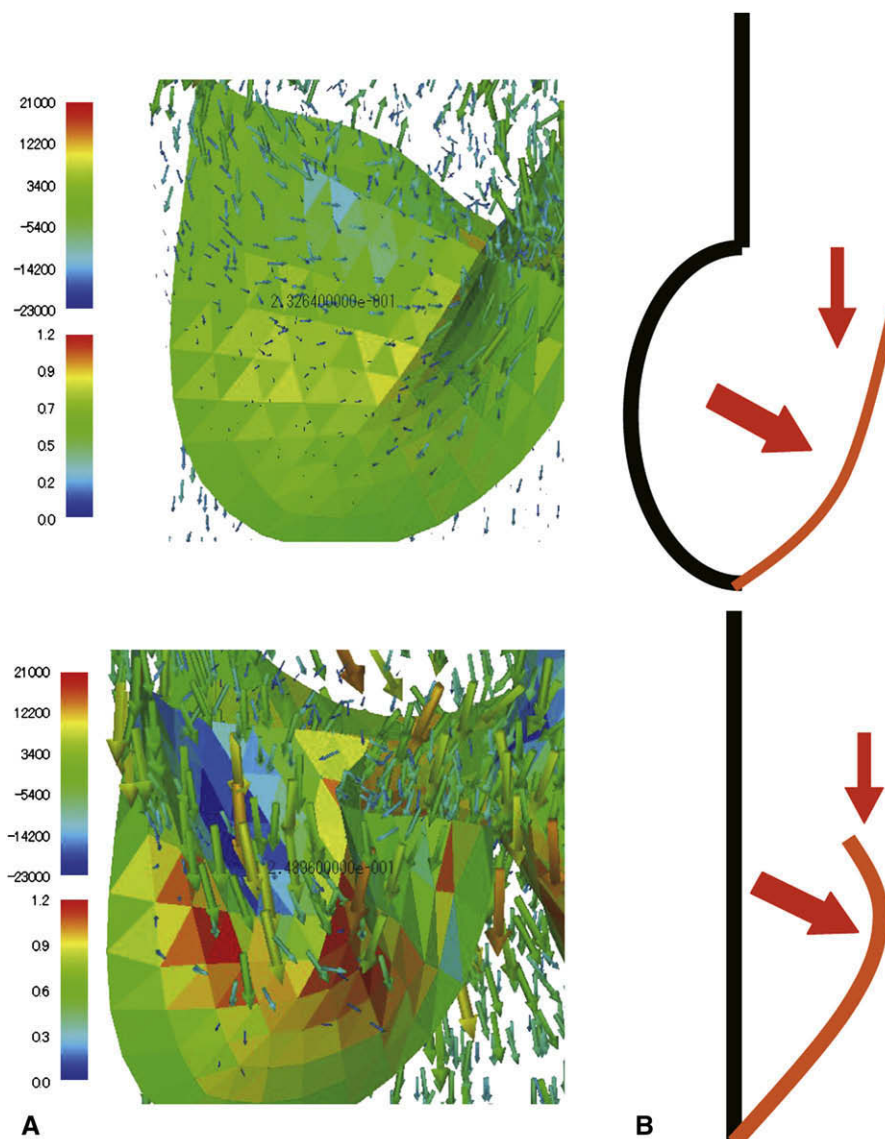


FIGURE 5. Stress in the leaflet and deformation. A, Close-up views of the leaflet in the late phase of ejection for pseudosinus (*upper panel*) and cylindrical (*lower panel*) models. Stress values shown in color coding indicate the higher stress in the cylindrical model. B, Schematic diagrams showing the direction of stress and induced deformation of the leaflets for pseudosinus (*upper panel*) and cylindrical (*lower panel*) models. Movies corresponding to this figure are available online.

orientation (Figure 5, B). So far, the stresses in the leaflet have been discussed mainly during diastole when leaflets are in the closed position, but the current simulation study demonstrated another important time point when abnormal stresses could build up, as well as the importance of fluid–structure interaction in consideration of designing the aortic root grafts.

Limitation of the Study

In this simulation, only the short segment of ascending aorta was modeled as a rigid tube. Furthermore, applied pressure and systemic circulation approximated by the 3-element Windkessel model are simplifications of the

real situation. These points should be improved to achieve more realistic and useful simulations. Use of clinical imaging data should also be considered. We are now working to model the entire thoracic aorta with realistic properties based on patients' computed tomographic data.

CONCLUSION

Sinuses of Valsalva facilitate the smooth closure of the aortic valve, thereby avoiding the building up of abnormal stress in the leaflet. With further improvement in modeling, the fluid–structure interaction analysis of aortic root dynamics can be a powerful tool for the optimum design of aortic root surgery.

References

1. van Steenhoven AA, van Dongen MEH. Model studies of the closing behavior of the aortic valve. *J Fluid Mech.* 1979;90:21-32.
2. Fung YC. How are the heart valves operated? Biomechanics, circulation. 2nd ed. New York: Springer-Verlag; 1997. p. 42-9.
3. Leyh RG, Schimidke C, Sievers H-H, Yacoub MH. Opening and closing characteristics of the aortic valve after different types of valve-preserving surgery. *Circulation.* 1999;100:2153-60.
4. de Oliveira NC, David TE, Ivanov J, Armstrong S, Eriksson MJ, Rakowski H, et al. Results of surgery for aortic root aneurysm in patients with Marfan syndrome. *J Thorac Cardiovasc Surg.* 2003;125:789-96.
5. David TE, Armstrong S, Ivanov J, Feindel CM, Omran A, Webb G. Results of aortic valve-sparing operations. *J Thorac Cardiovasc Surg.* 2001;122:39-46.
6. Demers P, Miller DC. Simple modification of 'T. David-V' valve-sparing aortic root replacement to create graft pseudosinuses. *Ann Thorac Surg.* 2004;78:1479-81.
7. Takamoto S, Nawata K, Morota T. A simple modification of 'David-V' aortic root reimplantation. *Eur J Cardiothorac Surg.* 2006;30:560-2.
8. De Paulis R, De Matteis GM, Nardi P, Scaffè R, Buratta MM, Chiariello L. Opening and closing characteristics of the aortic valve after valve-sparing procedure using a new aortic root conduit. *Ann Thorac Surg.* 2001;72:487-94.
9. De Paulis R, De Matteis GM, Nardi P, Raffaele S, Bassano C, Chiariello L. Analysis of valve motion after reimplantation type of valve-sparing procedure (David I) with a new aortic root conduit. *Ann Thorac Surg.* 2002;74:53-7.
10. Markl M, Draney MT, Miller DC, Levin JM, Williamson EE, Pelc NJ, et al. Time-resolving three-dimensional magnetic resonance velocity mapping of aortic flow in healthy volunteers and patients after valve-sparing aortic root replacement. *J Thorac Cardiovasc Surg.* 2005;130:456-63.
11. Fries R, Graeter T, Aicher D, Reul H, Schmitz C, Böhm M, et al. In vitro comparison of aortic valve movement after valve-preserving aortic replacement. *J Thorac Cardiovasc Surg.* 2006;132:32-7.
12. Erasmi A, Sievers H-H, Scharfshwerdt M, Eckel T, Misfeld M. In vitro hydrodynamics, cusp-bending deformation, and root distensibility for different types of aortic valve-sparing operations: remodeling, sinus prosthesis, and reimplantation. *J Thorac Cardiovasc Surg.* 2005;130:1044-9.
13. Grande-Allen KJ, Cochran RP, Reinhall PG, Kunzelman KS. Re-creation of sinuses is important for sparing the aortic valve: a finite element study. *J Thorac Cardiovasc Surg.* 2000;119:753-63.
14. Beck A, Thubrikar MJ, Robicsek F. Stress analysis of the aortic valve with and without the sinuses of valsalva. *J Heart Valve Dis.* 2001;10:1-11.
15. Nicosia MA, Cochran RP, Einstein DR, Rutland CJ, Kunzelman KS. A coupled fluid-structure finite element model of the aortic valve root. *J Heart Valve Dis.* 2003;12:781-9.
16. De Hart J, Peters GW, Schreurs PJ, Baaijens FP. A three-dimensional computational analysis of fluid-structure interaction in the aortic valve. *J Biomech.* 2003;36:103-12.
17. Zhang Q, Hisada T. Analysis of fluid-structure interaction problems with structural buckling and large domain changes by ALE finite element method. *Comput Methods Appl Mech Engrg.* 2001;190:6341-57.
18. Watanabe H, Hisada T, Sugiura S, Okada J, Fukunari H. Computer simulation of blood flow, left ventricular wall motion and their interrelationship by fluid-structure interaction finite element method. *JSME Internatl J C.* 2002;45:1003-12.
19. Watanabe H, Sugiura S, Hisada T. Finite element analysis on the relationship between left ventricular pump function and fiber structure within the wall. *JSME Internatl J C.* 2003;46:1330-9.
20. Watanabe H, Sugano T, Sugiura S, Hisada T. Finite element analysis of ventricular wall motion and intra-ventricular blood flow in heart with myocardial infarction. *JSME Internatl J C.* 2004;47:1019-26.
21. Watanabe H, Sugiura S, Hisada T. Multi-physics simulation of left ventricular filling dynamics using fluid-structure interaction finite element method. *Biophys J.* 2004;87:2074-85.
22. Swanson WM, Clark RE. Dimensions and geometric relationship of the human aortic valve as a function of pressure. *Circ Res.* 1974;35:871-82.
23. Sahasakul Y, Edwards WD, Naessens JM, Tajik AJ. Age-related changes in aortic and mitral valve thickness: implications for two-dimensional echocardiography based on an autopsy study of 200 normal human hearts. *Am J Cardiol.* 1988; 62:424-30.
24. Peskin CS, McQueen DM. A three-dimensional computational model for blood flow in the heart: I. Immersed elastic fibers in a viscous incompressible fluid. *J Comp Physiol.* 1989;81:372-405.
25. Cochran RP, Kunzelman KS, Eddy AC, Hofer BO, Verrier ED. Modified conduit preparation creates a pseudosinus in an aortic valve-sparing procedure for aneurysm of the ascending aorta. *J Thorac Cardiovasc Surg.* 1995;109:1049-58.
26. David TE. Aortic valve sparing operations. *Ann Thorac Surg.* 2002;73:1029-30.
27. David TE. *Commentary.* *J Thorac Cardiovasc Surg.* 2000;119:762-3.

TABLE E1. Material property of the valve

Elastic modulus in the fiber direction (E_L)	700 kPa
Elastic modulus perpendicular to the fiber direction (E_T)	233 kPa
Poisson's ratio (ν_{LT})	0.45
Shear modulus (G_{LT})	80 kPa